RSC Advances

ROYAL SOCIETY OF CHEMISTRY

www.rsc.org/advances

Giant piezoelectric properties of BZT-0.5BCT thin films induced by nanodomain structure

W.L. Li[a,b*], T.D. Zhang[a], Y.F. Hou[a], Y. Zhao[a], D. Xu[a], W.P. Cao[a], W.D. Fei[a,c]

a School of Materials Science and Engineering, Harbin Institute of Technology, Harbin 150001, P.R. China

b National Key Laboratory of Science and Technology on Precision Heat Processing of Metals, Harbin Institute of Technology, Harbin 150001, P.R. China

c State Key Laboratory of Advanced Welding and Joining, Harbin Institute of Technology, Harbin 150001, P. R. China

Abstract:

The $Ba(Zr_{0.2}Ti_{0.8})O_3$-$0.5(Ba_{0.7}Ca_{0.3})TiO_3$ (BZT-0.5BCT) thin films were prepared by two ceramics targets $Ba(Zr_{0.2}Ti_{0.8})O_3$ and $(Ba_{0.7}Ca_{0.3})TiO_3$ using a dual-magnetron sputtering, and $LaNiO_3$ (LNO) seed layer was introduced between the film and Pt(111)/Ti/SiO_2/Si substrates via the sol-gel technique. The domain structure has been performed on the thin films by piezoelectric force microscopy (PFM), and then autocorrelation function technique was applied to analyzing the obtained PFM images. The domain mean size of BZT-0.5BCT and (001)-oriented BZT-0.5BCT/LNO thin film is 69.2 nm and 151 nm at room temperature respectively. On the basis of our results, it is proved that the nanodomain has a deeply effect on piezoelectricity of thin films for MPB composition, the converse piezoelectric coefficient d_{33} is 258 pm/V of BZT-0.5BCT thin film and 122 pm/V of BZT-0.5BCT/LNO thin film. It is worth noting that not only the crystal orientation, but also the domain structures play critical roles in the piezoelectricity for BZT-0.5BCT thin film. Furthermore, (001)-oriented BZT-0.5BCT/LNO thin film exhibits excellent dielectric properties, the dielectric

* Corresponding author:
Prof. W.L. Li
School of Materials Science and Engineering,
Harbin 150001, P.R. China
E-mail: wlli@hit.edu.cn
Fax/Tel: +86-451-86415894

constant (ε~1046) is dramatically increased compared with BZT-0.5BCT thin film (ε~168). The *C-V* results indicate both of the thin films have ferroelectric nature.

Keywords: BZT-BCT films; $LaNiO_3$ seed layer; Nanodomain; Autocorrelation analysis; Piezoelectric properties.

Introduction

Lead-based compounds (PZT, PMN-PT)[1,2], which have been extensively applying in sensors, actuators, and energy harvesters[3], are the most popularly used piezoelectric materials, due to their excellent piezoelectric properties, While their wide applications have caused many environmental problems because of the strong toxicity of the high content of lead in these piezoelectric materials. Therefore, many efforts have been made to search lead-free candidates to replace lead-based ceramics and thin films. Recently, it was reported that $0.5Ba(Zr_{0.2}Ti_{0.8})O_3$-$0.5(Ba_{0.7}Ca_{0.3})TiO_3$ (abbreviated as BZT-0.5BCT) ceramic shows a surprisingly high piezoelectric coefficient of d_{33}~620 pC/N at morphotropic phase boundary (MPB)[4], which is considered to be one of the most important lead-free substitute that can be comparable with PZT.

BZT-xBCT thin films offer several advantages over its bulk counterparts, such as lower driving voltages and the potential for monolithic with Si, which have attracted much attention from the research community. Although both results of G.Q. Kang et al[5]. and A. Piorra et al[6]. indicate d_{33} of BZT-xBCT are less than 80 pm/V, which is smaller than that of PZT thin films (100~120 pm/V[7]), it is widely believed that

excellent piezoelectricity would be obtained at the MPB where no or lower energy barrier exists for the polarization rotation from *(001)T* to *(111)R* state[8]. Besides MPB, crystal orientation and domain structure of thin films are also important factors to piezoelectricity[9-12]. It is well known that oriented BZT-BCT piezoelectric thin films always show enhanced dielectric, ferroelectric and piezoelectric properties[9,13,14]. Furthermore, domain structure, especially their configuration, play a major role in ferroelectric switching in the ferroelectric and relaxor-ferroelectric materials[15]. However, there is little research on studying how domain structure and crystal orientation affect the piezoresponse of BZT-0.5BCT thin film up to now[14]. The piezoelectric force microscopy (PFM) has been successfully developed and subsequently used for the local characterization of piezoelectric materials on the nanometer scale, especially the static and dynamic polarization behavior in ferroelectrics. PFM can describe the polar nanosized regions (PNRs) or polar nanodomains (PNDs)[15,16].

In this study, the BZT-0.5BCT thin films were prepared by radio frequency dual-magnetron sputtering. With the help of PFM and autocorrelation technique, the domain structure, piezoresponse, converse piezoelectric coefficients d_{33} and dielectric properties of the BZT-0.5BCT thin films with and without (001) preferred orientation are discussed and analyzed.

Experimental

The $Ba(Zr_{0.2}Ti_{0.8})O_3$-$0.5(Ba_{0.7}Ca_{0.3})TiO_3$ thin films were prepared by two ceramics targets ($Ba(Zr_{0.2}Ti_{0.8})O_3$ and $(Ba_{0.7}Ca_{0.3})TiO_3$) using a dual-magnetron

sputtering. Prior to deposition, the targets were pre-sputtered for 10min to eliminate surface heterogeneity, and then sputtered under an RF power of 40 W at 500 □ in Ar and O_2 atmosphere with the pressure of 1.4 Pa.

$LaNiO_3$ (LNO) seed layer was grown on Pt(111)/Ti/SiO_2/Si substrates using a sol-gel process. The first processing step was to spin-coating a thin LNO layer onto the Pt/Ti/SiO_2/Si substrate followed by pyrolysis at 375 ℃ for 3 min, and then the seed layer was annealed at 750 ℃ for 30 min. Next, BZT-0.5BCT thin film was sputtered by off-axis RF magnetron sputtering on LNO/ Pt(111)/Ti/SiO_2/Si. Finally, the resulting films were heated at 750 ℃ for 30 min for crystallization. Before the performance testing, Platinum electrodes as the top electrode with a size of 3.14×10^{-4} cm^2 were deposited by a DC magnetron sputtering.

The crystalline structures of the thin films were analyzed by a Philips X' pert X-ray diffractometer (XRD) with Cu K_α radiation generated at 40 kV and 40 mA. We propose a universal fiber texture on the basis of ω-scan XRD. The cross-section micrograph of the thin film was performed by SEM (Helios Nanolab600i) and the surface morphology of the thin films was observed by atomic force microscopy (CSPM5600 of Benyuan). The piezoelectric properties of the thin films, including PFM images and piezoelectric constant, were observed by a commercial scanning force microscope (CSPM5600 of Benyuan) equipped with a lock-in amplifier (model SR530, Stanford Research Systems, Inc.). The PFM images measurements were performed in a piezoelectric contact mode, which are currently widely applied for the nanoscale characterization of domain structure. For domain visualization, the ac

voltage, amplitude 1 v and frequency 20 kHz, respectively, was applied between the grounded tip and bottom electrode. The piezoelectric constants of the samples were measured with poled ahead of time. In the poling process, the BZT-0.5BCT thin films were applied a voltage of 500 kV/cm for 10 min. For measurements of converse piezoelectric coefficients d_{33} in all films, the top platinum electrodes with the same size of $3.14\times10^{-4}cm^2$ were contacted with conductive tip. The input ac sine wave voltage, amplitude in the range of 0.5v~3v and frequency 5kHz which was chosen far away from resonant frequencies of the cantilever and acquiring the piezoelectric response during each pulse, respectively, was applied between the conductive tip and bottom electrode in the thickness direction. The corresponding vertical deflection signal of the cantilever is recorded by lock-in amplifier. By multiplying the deflection signal with the calibration constant of the photodetector sensitivity, the amplitude of the tip vibration was derived. Frequency dependence of dielectric permittivity and the capacitance-voltage of samples were measured using an Agilent 4294A precision impedance analyzer. The dielectric property measurement was performed at frequencies ranging from 10 kHz to 1 MHz. The capacitance-voltage property was measured with applied dc bias voltage from -10 v to 10 v.

Results and Discussion

The XRD diffraction patterns of BZT-0.5BCT and BZT-0.5BCT/LNO thin films show pure perovskite-type structure, there are no detectable impurity or secondary phases. As shown in the inset of Fig.1, A FWHM value of ω =8.1° measured at the (100) peak indicates (001)-orientated growth attributed to the lattice mismatch and

interfacial effect between LNO seed layer and BZT-BCT thin film.

Both of the films exhibit a uniform and denser surface structure as can be seen in Fig.2. The grain size is 150nm and 177nm for BZT-0.50BCT and BZT-0.50BCT/LNO thin films respectively. In addition, LNO seed layer has an obvious influence on the surface roughness of the thin films, viz., 5.2nm for the film with LNO seed layer, smaller than the one (9.8nm) without LNO seed layer. The SEM micrographs of the cross-section of films were given in Fig.2(c) and 2(d). The scanning results show that the thickness of the films is approximately 200nm and the films have a dense microstructure in the microscopic scale.

Fig.3 shows the representative PFM images measured on BZT-0.5BCT and BZT-0.5BCT /LNO thin films at room temperature. As shown in the Fig.3(a), it can be seen that the BZT-0.5BCT thin film is consists of nanodomains regions with up and down polarizations and the mesh-like structure with slim and bright boundaries. On total scale, the uniform distribution of the pattern of mesh-like structure PNRs indicates well short-range ferroelectric order. For the sake of avoiding the effect of external signal, we chosen the regions highlighted in black wireframe with the size of 1500 nm × 1500 nm for autocorrelation where can avoid the influence by scanning lines. In Fig.3(b), the PFM image of BZT-0.5BCT/LNO thin film has clearly visible grain boundaries and a clear contrast between opposite polarity was observed. The size of these piezoactive regions varies in the range from hundreds nanometers to micrometers, their distributions show disorder on a large scale and the higher limit of the distribution may be originated from the introduction of LNO seed layer, so we

chosen the microdomains regions for analysis as reported by V. V. Shvartsman[17]. The 3D autocorrelation images of BZT-0.5BCT and BZT-0.5BCT/LNO thin films, as shown in Fig.3(c) and Fig.3(d), were obtained from the original PFM via autocorrelation transformation:

$$C(r_1, r_2) = \sum_{x,y} D(x, y)D(x + r_1, y + r_2)$$

Where *D(x,y)* is the value of piezoresponse signal.

Autocorrelation analysis of the PFM data provided a quantitative insight into the polarization distribution and nanodomain structure. Autocorrelation analysis was applied to estimate the size of PNRs[18-20]. The autocorrelation function can be represented as a sum of two contributions:

$$C_{(r)} = A\exp[-(\frac{r}{\xi})^{2h}] + (1-A)\exp[-\frac{r}{r_c}]\cos(\frac{\pi r}{a})$$

The first term and second term corresponds to short range correlation and long range correlation, respectively. Only a short range correlation length term was taken into account for uniform morphology of thin films[20] and useful for the estimation of characteristic parameters of nanodomains. In this case, the experimental curves that obtained from the cross section of two-dimension autocorrelation images, as shown in Fig.(4), were approximated fitted with the first term:

$$C_{(r)} = A\exp[-(\frac{r}{\xi})^{2h}]$$

Here r is the distance from the central maximum, ξ represents short range correlation length, and h ($0<h<1$) is a parameter related to fractal dimension of "polarization interface". A is the normalization constant.

Fig.4(a) and Fig.4(b) show the $C_{(r)}$ at a small r averaged over all in-plane directions. The short correlation length ξ, which is estimated from the best fit to $C_{(r)}$, is 69.2 nm of BZT-0.5BCT thin film and 151 nm of BZT-0.5BCT/LNO thin film, respectively. It indicates that the mean size of nanodomains of BZT-0.5BCT/LNO thin film is more than twice as large as that of the BZT-0.5BCT thin film. The larger size of the PNRs is due to stronger polar correlations in the thin film with LNO seed layer. Furthermore, the interface induced by LNO seed layer is more conductive to nucleation and aggregation for large nanodomain of thin films.

As shown in Fig.5, both BZT-0.5BCT and BZT-0.5BCT/LNO thin films exhibit excellent piezoelectricity at room temperature, converse piezoelectric coefficient d_{33} are 258 pm/V and 122 pm/V, respectively, higher than 71.7 pm/V[5], 80 pm/V[6] and 100 pm/V[9]. The composition of BZT-0.5BCT thin film is located at MPB which has low potential barrier for polarization rotation from *(001)T* state to *(111)R* state at room temperature[8], it gives rise to the outstanding piezoeletricity. Meanwhile, the encouraging results of BZT-0.5BCT thin film without LNO seed layer may be attributed to smaller nanodomain structure, domains state[21] and the existence of non-180° domain[9] in the random oriented-BZT-0.5BCT thin film which enable more easily polarization rotation than the larger nanodomains of (001)-oriented BZT-0.5BCT/LNO thin film under the same external stimulation. The insertion of LNO seed layer may provide nucleation sites and reduce the activation energy for BZT-0.5BCT thin films, resulting in the better crystallization and the enhancement of piezoelectric constant.

The dielectric properties of BZT-0.5BCT thin films were measured at room temperature as a function of frequency ranging from 10 kHz to 1 MHz and given in Fig.6(a) and Fig.6(b). The BZT-0.5BCT and BZT-0.5BCT/LNO thin film show the largest dielectric permittivity of 168 and 1064 at the frequency of 1 MHz. The dielectric loss of the films at 1 MHz are as low as 0.076 and 0.37. Fig.6(c) and Fig.6(d) show capacitance-voltage (*C-V*) characteristics of the BZT-0.5BCT and BZT-0.5BCT/LNO thin films at room temperature and at the frequency of 1 MHz. The maximum capacitance value of BZT-0.5BCT and BZT-0.5BCT/LNO thin films are 233 pF and 869 pF. The (001)-oriented BZT-0.5BCT/LNO film can manifest the more excellent dielectric properties compared with the BZT-0.5BCT thin film, because the spontaneous polarization vector points are normal to the (001)-oriented film surface and coincides with the dielectric measuring direction. The films' butterfly-shaped (*C-V*) curves which caused by switching of the ferroelectric domains indicate that the films have ferroelectric nature[22]. The curves are slightly asymmetrical on either side of the two branches, which may be attributed to the asymmetrical distribution of the space charge, oxygen vacancies[13] and the introduction of LNO seed layer.

Conclusion

In summary, the BZT-0.5BCT and BZT-0.5BCT/LNO thin films were prepared by two ceramics targets $Ba(Zr_{0.2}Ti_{0.8})O_3$ and $(Ba_{0.7}Ca_{0.3})TiO_3$ using a dual-magnetron sputtering. The better crystallization and orientation of BZT-0.5BCT/LNO thin film, which is caused by the insertion of LNO seed layer, lead to the relatively higher

piezoelectric coefficient (122 pm/V). The great converse piezoelectric coefficient ~258 pm/V is attributed to the smaller nanodomain size ~69.2 nm of the BZT-0.5BCT thin film. By comparison of the piezoelectricity of BZT-0.5BCT and BZT-0.5BCT/LNO thin films, it can been seen that the nanodomain structure rather than the crystal orientation has a more significantly effect on the converse piezoelectric coefficient. Meanwhile, the crystal orientation is also conductive to the dielectric properties of BZT-0.5BCT thin films for MPB composition. With the excellent piezoelectric property, the non-Pb system BZT-BCT films are potential candidates for the lead-free piezoelectric applications.

Acknowledgment: The authors gratefully acknowledge support from Natural Science Foundation of China (Grant Nos. 11272102 and 51202049)

References:

[1] Gun-Tae Park, Jong-Jin Choi, Jungho Ryu, H. G. Fan and Hyoun-Ee Kim, Appl. Phys. Lett. 80, 4606 (2002).

[2] V. V. Shvartsman, A. L. Kholkin, I. P. Raevski, S. I.. Raevskaya, F. I. Savenko and A. S. Emelyanov, Appl. Phys. Lett. 113, 187208 (2003).

[3] Elena Aksel and Jacob L.Jones, Sensors. 10, 1935-1954 (2004).

[4] H. X. Bao, C. Zh, D. Z. Xue, J. H. Gao and X. B. Ren, J. Phys. D: Appl. Phys. 43, 465401 (2010).

[5] G. Q. Kang, K. Yao and John, Wang, J. Am. Ceram. Soc. 1-6 (2011).

[6] A. Piorra, A. Petraru, H. Kohlstedt, M. Wuttig, and E. Quandt, J. Appl. Phys. 109 104101-1 (2011).

[7] N. Ledermann, P. Muralt, J. Baborowski, S. Gentil, K. Mukati, M. Cantoni, A. Seifert, and N. Setter, Sens. Actuators, A105, 162-170 (2003).

[8] W. F. Liu and X. B. Ren, Phys. Rev. Lett. 103, 257602-2 (2009).

[9] B. C. Luo, D. Y. Wang, M. M. Duan and S. Li, Appl. Phys. Lett. 103, 122903 (2013).

[10] V. V. Shvartsman, A. L. Kholkin, M. Tyunina and J. Levoska, Appl. Phys. Lett. 86, 222907 (2005).

[11] N. A. Pertsev, A. Petraru, H. Kohlstedt, R. Waser, I. K. Bdikin, D. Kiselev and A. L. Kholkin, Nanotechnology. 19, 375703 (2008).

[12] V. V. Shvartsman, A. L. Kholkin, Phys. Rev. B. 69, 014102 (2004).

[13] W. Li, J. G. Hao, W. F. Bai and J. W. Zhai, J. Sol-Gel Sci Technol. 66, 220-224

(2013).

[14] B. C. Luo, D. Y. Wang, M. M. Duan and S. Li, Applied Surface Science. 270, 377-381 (2013).

[15] H. Uršič, J. Ricote, H. Amorín, J. Holc, M. Kosec and M. Algueró, J. Phys. D: Appl. Phys. 45, 265402 (2012).

[16] X. Zhao, J. Y. Dai, J. Wang, H. L. W. Chan and C. L. Choy, Phys. Rev. B. 72, 064114 (2005).

[17] V. V. Shvartsman, A. L. Kholkin, Appl. Phys. Lett. 86, 202907 (2005).

[18] V. V. Shvartsman, A. L. Kholkin, Appl. Phys. Lett. 101, 064108 (2007).

[19] P. Sharma, T. Reece, D. W. Wu, V. M. Fridkin and S. Ducharme and A. Gruverman, J. Phys: Condens. Matter21, 485902 (2009).

[20] V. V. Shvartsman, B. Dkhil, A. L. Kholkin, Annu. Rev. Mater, Res. 43:423-49 (2013).

[21] H. X. Fu and R. E. Cohen, Nature. 403: 281 (2000).

[22] H. Basantakumar Sharma, Ferroelectrics. 453:113-121 (2013).

Captures

Fig.1. XRD patterns of BZT-0.5BCT thin film without LNO seed layer and BZT-0.5BCT thin film with LNO seed layer, inset shows the XRD ω-scan for the (001)-oriented BZT-0.5BCT thin film with LNO seed layer.

Fig.2 AFM images of BZT-0.50BCT thin films (a) without LNO seed layer and (b) with LNO seed layer；SEM images of BZT-0.50BCT thin films (c) without LNO seed layer and (d) with LNO seed layer.

Fig.3 PFM and autocorrelation images of BZT-0.50BCT thin films (a) PFM image of thin film without LNO seed layer and (b) PFM image of thin film with LNO seed layer; (c) autocorrelation image of thin film without LNO seed layer and (d) autocorrelation image of thin film with LNO seed layer.

Fig.4 Distance (r) dependence of the auto-correlation function ($C_{(r)}$), averaged over all in-plane directions for Fig.4(a) corresponds to the 3D autocorrelation image in Fig.3(c), Fig.4(b) corresponds to the 3D autocorrelation image in Fig.3(d).

Fig.5 Linear fit of experimental data for converse piezoelectric coefficients d_{33} of BZT-0.5BCT thin film (a) without LNO seed layer and (b) with LNO seed layer.

Fig.6 Frequency dependence of dielectric permittivity and dielectric loss for BZT-0.5BCT thin films (a) without LNO seed layer and (b) with LNO seed layer;

C-V curves of BZT-0.5BCT thin films at the frequency of 1MHz (c) without LNO seed layer and (d) with LNO seed layer.

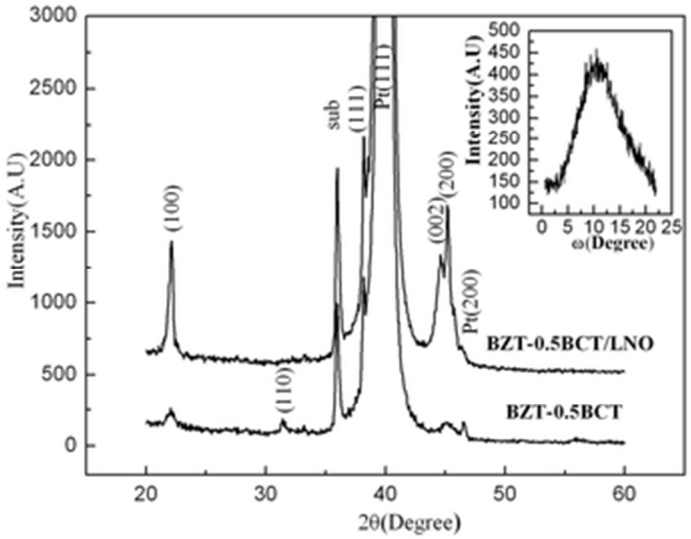

Fig.1. XRD patterns of BZT-0.5BCT thin film without LNO seed layer and BZT-0.5BCT thin film with LNO seed layer, inset shows the XRD ω-scan for the (001)-oriented BZT-0.5BCT thin film with LNO seed layer.
30x22mm (300 x 300 DPI)

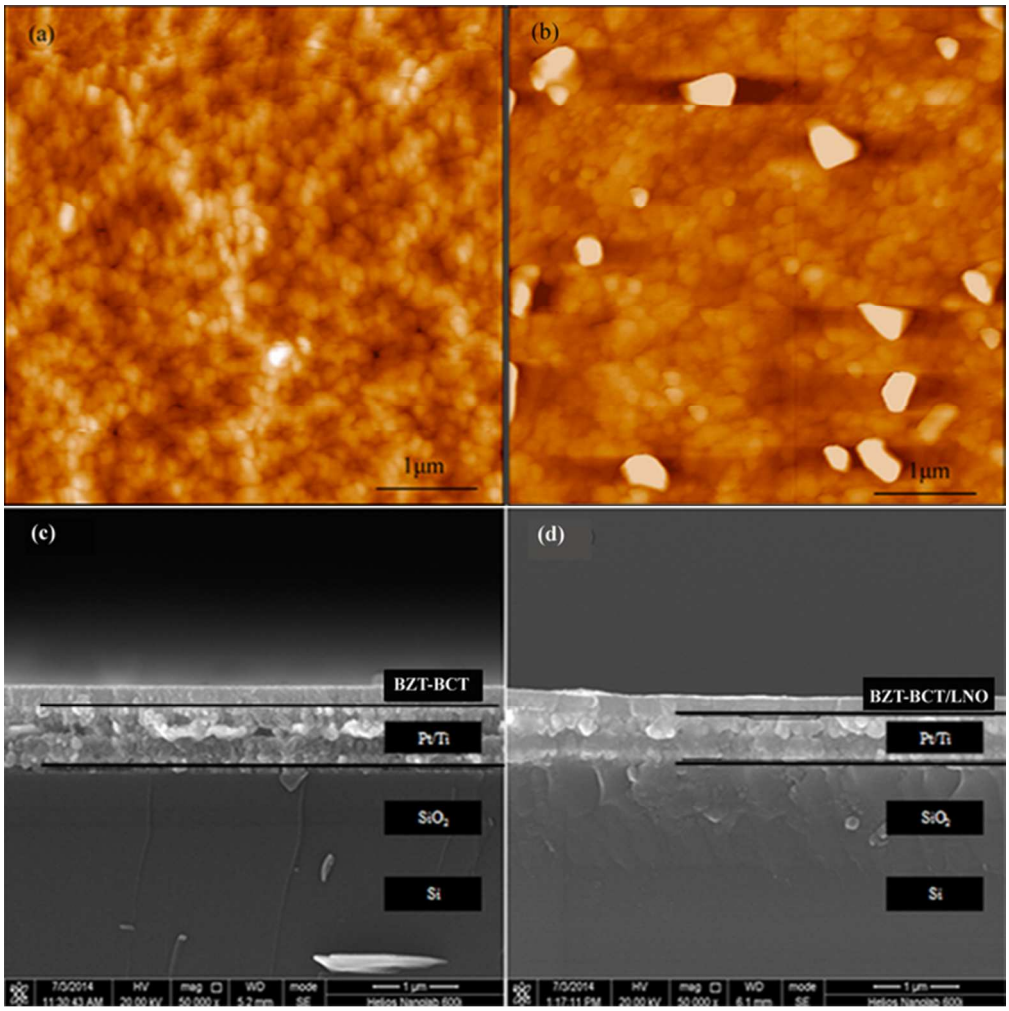

Fig.2 AFM images of BZT-0.50BCT thin films (a) without LNO seed layer and (b) with LNO seed layer ; SEM images of BZT-0.50BCT thin films (c) without LNO seed layer and (d) with LNO seed layer.
59x59mm (300 x 300 DPI)

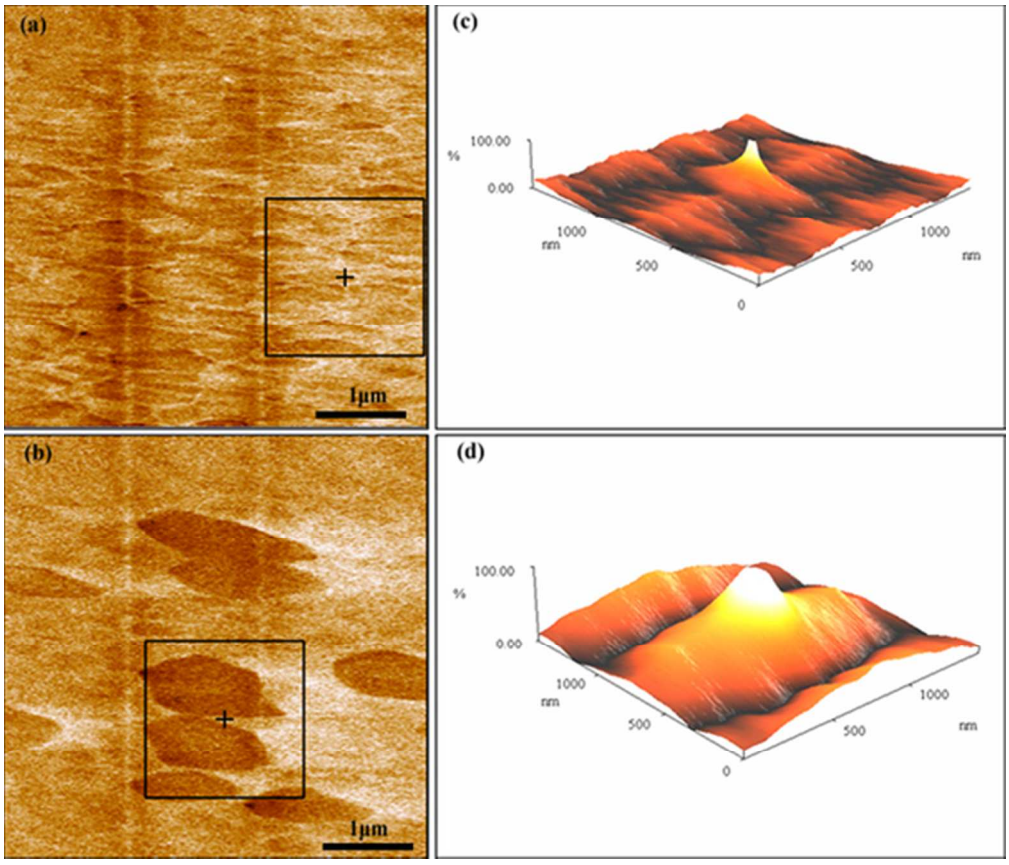

Fig.3 PFM and autocorrelation images of BZT-0.50BCT thin films (a) PFM image of thin film without LNO seed layer and (b) PFM image of thin film with LNO seed layer; (c) autocorrelation image of thin film without LNO seed layer and (d) autocorrelation image of thin film with LNO seed layer.
51x43mm (300 x 300 DPI)

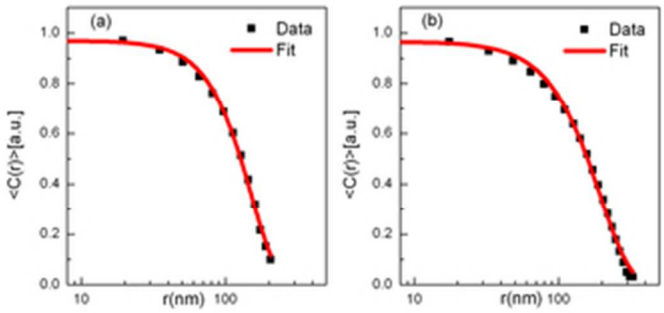

Fig.4 Distance (r) dependence of the auto-correlation function (C(r)), averaged over all in-plane directions for Fig.4(a) corresponds to the 3D autocorrelation image in Fig.3(c), Fig.4(b) corresponds to the 3D autocorrelation image in Fig.3(d).
28x13mm (300 x 300 DPI)

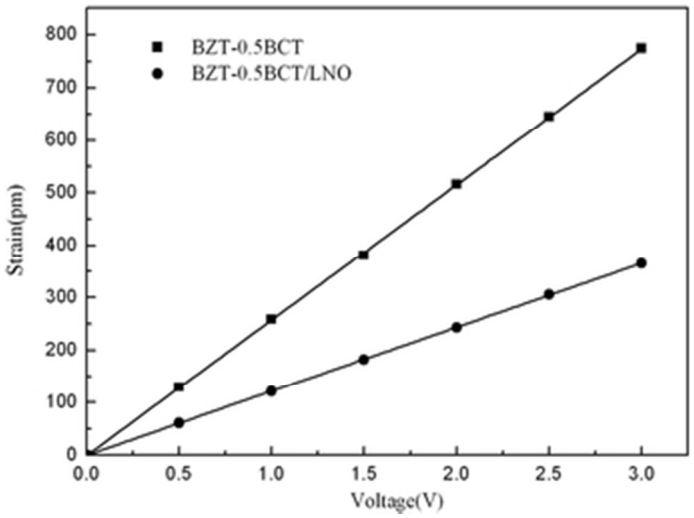

Fig.5 Linear fit of experimental data for converse piezoelectric coefficients d33 of BZT-0.5BCT thin film (a) without LNO seed layer and (b) with LNO seed layer.
29x21mm (300 x 300 DPI)

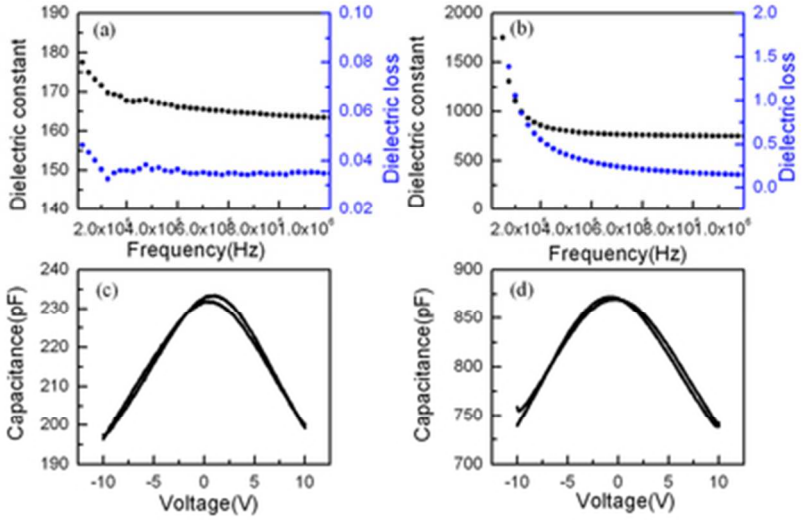

Fig.6 Frequency dependence of dielectric permittivity and dielectric loss for BZT-0.5BCT thin films (a) without LNO seed layer and (b) with LNO seed layer; C-V curves of BZT-0.5BCT thin films at the frequency of 1MHz (c) without LNO seed layer and (d) with LNO seed layer.
35x22mm (300 x 300 DPI)